IEEE Photonics Journal
An IEEE Photonics Society Publication

Open Access

Stress-Induced Refractive Index Changes in Laser Fibers and Preforms

(Invited Paper)

Volume 11, Number 6, December 2019

Pauli Kiiveri
Joona Koponen
Juha Harra
Ossi Kimmelma
Jijo Paul
Ville Aallos
Steffen Novotny
Hannu Husu
Heikki Ihalainen

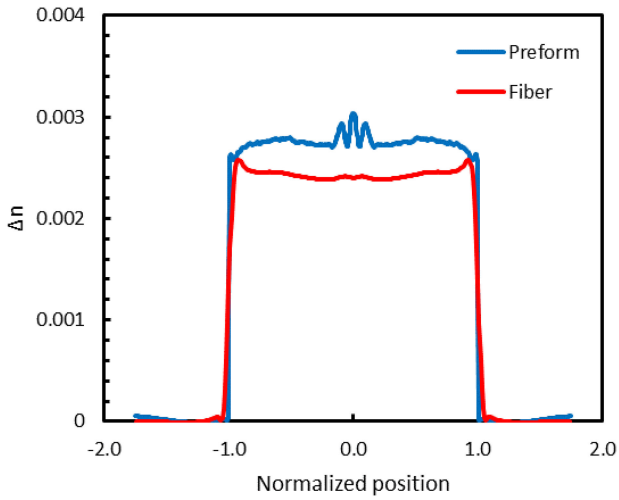

DOI: 10.1109/JPHOT.2019.2943208

IEEE photonics SOCIETY

IEEE

Stress-Induced Refractive Index Changes in Laser Fibers and Preforms

(Invited Paper)

Pauli Kiiveri, Joona Koponen, Juha Harra, Ossi Kimmelma, Jijo Paul, Ville Aallos, Steffen Novotny, Hannu Husu, and Heikki Ihalainen

The authors are with R&D, nLIGHT Corporation Lohja, 08500 Lohja, Finland

DOI:10.1109/JPHOT.2019.2943208

Manuscript received July 31, 2019; revised September 11, 2019; accepted September 17, 2019. Date of publication September 23, 2019; date of current version November 26, 2019. Corresponding author: Pauli Kiiveri (email: pauli.kiiveri@nLight.net).

Abstract: Refractive index profile of the core is a key design parameter in fiber lasers and amplifiers. During manufacturing, the initial information of the index profile is obtained from the preform, while ultimately the performance is defined by the index profile of the fiber. Depending on stresses and diffusion, the two profiles may be different. It is possible to predict more accurately the laser fiber refractive index when we apply a stress-induced index change model to the measured preform index profile data. The improved capability to predict the fiber index from preform increases the confidence in achieving the designed index profile in fiber, which enables faster process feedback and higher fiber yields.

Index Terms: Refractive index change, laser fiber, stress, optical fiber, preform, thermal stress, tension, modelling, DND.

1. Introduction

The refractive index difference values of active fibers and preforms are determined by the core composition but also influenced by the stress-induced index changes in the preforms and fibers. A refractive index value, measured from a preform, can change during the process steps that follow the preform manufacturing caused by changes in the residual stresses in the glass [1].

Repeatable preform manufacturing processes, such as direct nanoparticle deposition (DND) [2]–[4], allows analysing slight changes in the refractive index profiles. Better understanding of the stress-induced index changes helps to design high power large mode area (LMA) fibers that require accurate index profiles. To estimate stresses in glass materials, we need to know the transition temperatures, material composition, thermal expansion coefficients, preform and fiber dimensions, elastic modulus and viscosity of the doped and undoped glass.

In this article, we will present a simplified model to estimate the stresses and refractive index changes in the laser fibers and preforms. We apply thermal expansion coefficients, elastic modulus and viscosity as material parameters in the model. For doped silica, we calculate the material parameter values by linearly mixing the parameter values of pure dopant materials and silica. These doped material parameter values are applied to calculate the stresses. The stress-optical model is then used to predict the refractive index changes [1].

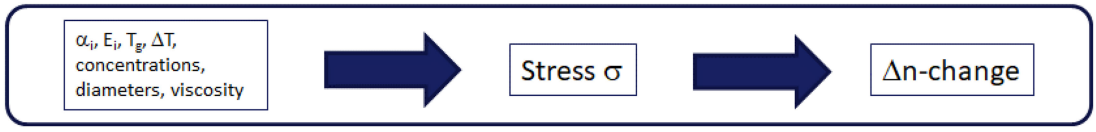

Fig. 1. Modelling steps for predicting stress-induced refractive index changes. Here α_i is the thermal expansion coefficient value, E_i the elastic modulus value, ΔT temperature change and T_g glass transition temperature. Diameters refer to the core and cladding diameters.

The stress-induced index change model allows estimating the refractive index changes when the glass composition and dimensions are varied. The model gives us a physical insight into the index change phenomenon and removes the limits set by the measurement data in statistical models [5].

2. Need for a Physical Model

We have earlier studied statistical correlations of the refractive index changes between the preform and fiber index values [5]. A linear model was created that predicts the index changes using statistical correlations between process parameters and measured refractive index changes. Statistical models are valid only in the range of available measurement data. Each fiber type needs its own set of modelling parameter values, and the statistical models have no direct physical basis. Thus, they have limited applicability in new fiber designs.

We will first build a model that estimates the stress-induced refractive index changes in preforms. It is based on dopant materials, glass composition, preform geometry and glass transition temperatures. For the fiber stresses, a similar model combined with drawing tension and viscosities is used. The preform and fiber stress models are used together to predict the index change between the preform and fiber measurements. The combination of the models will give us a physical insight of the index change phenomenon. The combined model can be used also for new fiber designs.

3. Modelling Steps and Material Parameters

The modelling steps for the thermally induced refractive index changes are shown in Fig. 1. The first task is to find out the correct material parameter values for the pure amorphous glass materials that are used to dope the silica. Knowing the material parameter values, we can calculate the thermal stresses in the glass. When the stress values are known, we can apply the stress-optical theory and calculate the stress-induced index change in the glass.

3.1 Average Thermal Expansion Coefficient and Elastic Modulus Values of Pure Oxides

Thermal expansion coefficient (TEC) values (α_i) and elastic modulus values (E_i) of doped silica glass (i) depend on temperature and dopant concentrations. The values of thermal expansion coefficients of pure amorphous oxides as a function of temperature can be found e.g., in references [6]–[13]. If we know the thermal expansion coefficient values (α_i) of the oxides, the TEC values of doped SiO_2 glass can be calculated by linear mixing of the coefficients values of pure oxides [14]. One must be aware that a simple linear additivity model is not valid for all material combinations [15]. In some cases, more complicated models are needed for combining material parameters. According to the ref. [15] (by Just *et al.*) a linear additivity is not valid for Al_2O_3-P_2O_5 in SiO_2 glass. There is a discontinuity in the refractive index and thermal expansion in dependence on the dopant concentration at a molar ratio of one.

We will apply temperature averaged, i.e., effective values of the thermal expansion and elastic modulus values of pure oxides instead of temperature-dependent values. This will simplify our stress models. The effective values α_i and E_i of the $\alpha_i(T)$ and $E_i(T)$ are calculated between the room

temperature T_0 and glass transition temperature T_g using Eq. (1):

$$\alpha_i = \int_{T_0}^{T_g} \frac{\alpha_i(T)}{(T_g - T_0)} dT \quad \text{and} \quad E_i = \int_{T_0}^{T_g} \frac{E_i(T)}{(T_g - T_0)} dT \tag{1}$$

The glass transition temperature T_g of the doped core is selected as the highest temperature in the averaging because the core behaves inelastically at higher temperatures. Stresses start to create during cooling when the core starts to behave elastically. In this study, the average TEC and elastic modulus values were calculated between 23 °C and 1150 °C for different glass materials using the data given in references [6]–[19]. The calculated effective values are:

Material	**TEC/°C^{-1}**	**Ref.**
Yb_2O_3	$3.85 \cdot 10^{-5}$	9, 10
Al_2O_3	$1.05 \cdot 10^{-5}$	8
SiO_2	$4.84 \cdot 10^{-7}$	6, 7, 11

Material	**Elastic modulus/GPa**	**Ref.**
Yb_2O_3	173.5	16
Al_2O_3	162	16, 17
SiO_2	84.4	18, 19

Slightly different effective values for α and E will be calculated if other data sources than those referred here, are used.

In principle, one can calculate the glass transition temperature of the core (T_{gco}) separately for each core material composition, but in practice the T_{gco} values do not vary much at typical dopant levels, and in this work, we have assumed a value of $T_{gco} = 1150$ °C for all core material compositions.

3.2 Thermal Expansion Coefficient of Doped Silica Glass

A TEC value (α_{mix}) of the doped silica glass is a combination of the effective TEC values α_i of the pure oxides. The TEC value of the doped glass is calculated using the concentrations of the glass component materials in vol% [14]. The thermal expansion coefficient α_{mix} of the doped SiO_2 glass is calculated as:

$$\alpha_{mix} = \sum_i c_i \cdot x_i \cdot \alpha_i \tag{2}$$

where

α_{mix} = TEC of doped silica glass
c_i = material dependent coefficient, e.g., $c_{Si} = c_{Yb} = 1$; $c_{Al} = 2$ as given by Cavillon in [14]:
x_i = concentration of a pure glass material i (in vol%)
α_i = effective TEC of a pure glass oxide i (dopant or silica), defined in Eq. (1).

The coefficients for the materials Yb_2O_3, Al_2O_3 and SiO_2 are given, because they are commonly used in Yb-doped laser fibers. A list of the c-parameters for some other fiber materials can be found in the reference [14] (by Cavillon *et. al.*).

3.3 Elastic Modulus of Doped Silica Glass

The solid material will deform when a load is applied to it. If the material returns to its original shape after the load is removed, the phenomenon is called elastic deformation. Elastic modulus, also known as Young's modulus, is a measure of the stiffness of the solid material. Elastic modulus depends on temperature and defines the relationship between stress and strain in a material.

Similarly, as we did with the TEC values, we can calculate the elastic modulus value E_{mix} of doped silica glass by mixing the effective E_i coefficients (Eq. (1)) of the pure glass materials:

$$E_{mix} = \sum_i x_i \cdot E_i \tag{3}$$

where

E_{mix} = elastic modulus of doped silica glass
x_i = concentration of a pure glass oxide i (in mol%)
E_i = effective elastic modulus of a pure glass oxide i (dopant or silica), defined in Eq. (1).

Elastic modulus values of the pure oxides can be found e.g., in ref. [16], [17] as a function of temperature.

4. Thermal Stress Model for Preforms and Fibers

Tension and stress can be caused by external forces, varying thermal expansion coefficient and elastic modulus values in the glass, and spatially varying temperature. Thermal stresses depend only on the material composition, glass geometry and temperatures.

4.1 Assumptions in the Thermal Stress Models

We will assume the cylindrical symmetry of the glass, radially constant doping profiles in the core, and low diffusion of dopant materials [20] during the process steps that follow the refractive index measurement of the preform. Also, only the index changes due to the radial stress affecting the LP_{01} mode are considered. For the higher order modes, the model would be more complicated, and we will not study it here.

Dopants change the thermal expansion coefficient and elastic modulus values of the SiO_2 glass. When the preform or fiber is heated and cooled, differently doped areas induce stresses in the glass structure.

4.2 Axial and Radial Thermal Stresses

The radial average (α_{ave}) of the effective thermal expansion coefficient $\alpha(r)$, over the whole core-cladding area, can be calculated as [1], [21]:

$$\alpha_{ave} = \frac{\int_0^{r_{cl}} \alpha(r) r \cdot dr}{\int_0^{r_{cl}} r \cdot dr} \tag{4}$$

If we insert the effective thermal expansion coefficient $\alpha(r) = \begin{cases} \alpha_{co}, & \text{when } r \le r_{co} \\ \alpha_{cl}, & \text{when } r > r_{co} \end{cases}$ in Eq. (4), this will yield:

$$\begin{aligned} \alpha_{ave} &= \frac{2}{r_{cl}^2} \int_0^{r_{cl}} \alpha(r) \cdot r \cdot dr \\ &= \frac{2}{r_{cl}^2} \int_0^{r_{co}} \alpha(r) \cdot r \cdot dr + \frac{2}{r_{cl}^2} \int_{r_{co}}^{r_{cl}} \alpha(r) \cdot r \cdot dr \\ &= \frac{r_{co}^2}{r_{cl}^2} \alpha_{co} + \left(1 - \frac{r_{co}^2}{r_{cl}^2}\right) \alpha_{cl} \end{aligned} \tag{5}$$

The values of the thermal expansion coefficients in the core α_{co} and cladding α_{cl} in Eq. (5) are: $\alpha_{co} = \alpha_{mix}$ and $\alpha_{cl} = \alpha_{SiO2}$. Using the radially averaged value α_{ave} in Eq. (5) as the TEC reference level, the axial thermal stress $\sigma_z(r)$ can be calculated in a preform and in a fiber [1], [22], [23]

with:

$$\sigma_z(r) = \int_{T_0}^{T_g} \frac{E(r)}{1-\nu} [\alpha(r) - \alpha_{ave}] \cdot dT$$
$$= \frac{\Delta T \cdot E(r)}{1-\nu} \left[\alpha(r) - \frac{r_{co}^2}{r_{cl}^2} \alpha_{co} - \left(1 - \frac{r_{co}^2}{r_{cl}^2}\right) \alpha_{cl} \right] \quad (6)$$

In Eq. (4-6), the symbols are:

$\Delta T = T_g - T_0$, temperature change,
$\alpha(r)$ = effective thermal expansion coefficient,
E(r) = effective elastic modulus value,
r = radial coordinate,
r_{co} = radius of the core in a preform or fiber,
r_{cl} = radius of the cladding in a preform or fiber,
ν = Poisson's ratio of SiO_2 (averaged from T_0 to T_g),
α_{ave} = radial average of the TEC,
σ_z = axial stress.

The value of the Poisson ratio ν is expected to vary only a little as a function of the dopant concentrations, thus the thermally averaged value of SiO_2 is used for doped glass. The $\alpha(r)$, E(r) and ν are the temperature averaged values and thus do not anymore depend on the temperature in Eq. (6).

We are interested in the changes in the radial stress $\sigma_r(r)$, because it changes the refractive index of the radially vibrating electrical field of the LP_{01} mode [10]. Radial stress $\sigma_r(r)$ at the position r is related to the axial stress $\sigma_z(r)$ by [1], [23]:

$$\sigma_r(r) = \frac{1}{r^2} \int_0^r \sigma_z(r)\, r \cdot dr \quad (7)$$

Tangential thermal stress $\sigma_\theta(r)$ is related to the axial and radial stresses by [1], [24]:

$$\sigma_\theta(r) = \sigma_z(r) - \sigma_r(r) \quad (8)$$

The approximation that the TEC is constant in the core area, ($\alpha(r) = \alpha_{co}$), implies via Eq. (6) that also the radial stress σ_z is constant in the core. Inserting the constant σ_z from Eq. (6) into Eq. (7) and integrating over the core radius in Eq. (7) gives us the average radial thermal stress σ_{rco} in the preform or fiber core:

$$\sigma_{rco} = \frac{1}{r_{co}^2} \frac{\Delta T \cdot E_{co}}{(1-\nu)} \int_0^{r_{co}} \left[\alpha(r) - \left(\frac{r_{co}^2}{r_{cl}^2} \alpha_{co} + \left(1 - \frac{r_{co}^2}{r_{cl}^2}\right) \alpha_{cl} \right) \right] \cdot r \cdot dr$$
$$= \frac{1}{r_{co}^2} \frac{\Delta T \cdot E_{co}}{(1-\nu)} \left(\alpha_{co} - \frac{r_{co}^2}{r_{cl}^2} \alpha_{co} - \left(1 - \frac{r_{co}^2}{r_{cl}^2}\right) \alpha_{cl} \right) \cdot \frac{1}{2} r_{co}^2$$

Thus, the radial thermal stress in the preform or fiber core is:

$$\sigma_{rco} = \frac{\Delta T \cdot E_{co}}{2(1-\nu)} \left(1 - \frac{r_{co}^2}{r_{cl}^2}\right) (\alpha_{co} - \alpha_{cl}), \quad (9)$$

where

$\Delta T = T_g - T_0$ is the temperature change,
r_{co} = preform or fiber core radius,
r_{cl} = preform or fiber cladding radius,
α_{co} = TEC of the core material,
E_{co} = elastic modulus of the core material,
α_{cl} = TEC of the cladding material.

5. Thermal Stress-Induced Index Changes

5.1 Tensile and Compressive Stresses Change the Refractive Index

If the external force applied to a glass material stretches (elongates) the material, then the related stress is called tension. Tension has positive values. Tensile stress decreases the refractive index of the glass, so the induced Δn change is negative.

If the external force is compressive, the result is called stress, and it has negative values. Compressive stress increases the refractive index of the glass, so the induced Δn change is positive. However, it is good to notice that the word *stress* is also used in a general meaning covering both tensile and compressive stresses (like in the main title of this article).

5.2 Stress-Optical Theory for Refractive Index Changes

The index change caused by stresses is calculated using the stress-optical theory. It applies the stress-optic coefficients C_1 and C_2 with the values $C_1 = 6.5 \cdot 10^{-7}$ MPa^{-1} and $C_2 = 4.2 \cdot 10^{-6}$ MPa^{-1} for SiO_2 glass [10]. By using the same values of C_1 and C_2 also for the doped glass, we can calculate the three components of the stress-induced index change in the preform and in the fiber core [1]:

$$n_r = n - C_1 \times \sigma_r - C_2 \times (\sigma_\theta + \sigma_z), \tag{10}$$

$$n_\theta = n - C_1 \times \sigma_\theta - C_2 \times (\sigma_r + \sigma_z), \tag{11}$$

$$n_z = n - C_1 \times \sigma_z - C_2 \times (\sigma_r + \sigma_\theta), \tag{12}$$

where

n = refractive index of unstressed glass,
n_r = radial refractive index,
n_θ = tangential refractive index,
n_z = axial refractive index,
σ_r = radial stress component,
σ_θ = tangential stress component,
σ_z = axial stress component.

Inserting the tangential stress component σ_θ from Eq. (8) into Eq. (10) gives:

$$\Delta n_r = n_r - n = (C_2 - C_1) \times \sigma_r - 2 \times C_2 \sigma_z \tag{13}$$

We will approximate the axial stress $\sigma_z(r)$ in the core area with the radially averaged value $\sigma_z(r) = \sigma_z$. Then, inserting this constant σ_z into Eq. (7) and integrating over the radius gives us the radial stress value $\sigma_r(r)$ in the core:

$$\sigma_r(r) = 1/2 \times \sigma_z \tag{14}$$

We can now calculate the radial index change Δn_r as a function of radial or axial stresses. Inserting σ_r from Eq. (14) into Eq. (13) gives the radial index change in the core as a function of the axial stress [25]:

$$\begin{aligned} \Delta n_r &= (C_2 - C_1) \times \sigma_r - 2 \cdot C_2 \times \sigma_z = -1/2 \cdot C_1 \times \sigma_z - 3/2 \cdot C_2 \times \sigma_z \\ &= -1/2 \times (C_1 + 3C_2) \times \sigma_z \end{aligned} \tag{15}$$

Similarly, inserting the axial stress component σ_z from Eq. (14) into (15) will give the radial index change as a function of radial stress as:

$$\Delta n_r = -(C_1 + 3C_2) \times \sigma_r \tag{16}$$

In the core area, the radial stress-induced average index change Δn_{co} is:

$$\Delta n_{co} = -(C_1 + 3C_2) \times \sigma_{rco} \tag{17}$$

Inserting the values of the stress-optic constants $C_1 = 6.5 \cdot 10^{-7}$ MPa^{-1} and $C_2 = 4.2 \cdot 10^{-6}$ MPa^{-1} into (17) gives:

$$\Delta n_{co} = -13.25 \cdot 10^{-6} \text{MPa}^{-1} \times \sigma_{rco}$$

and using Eq. (9) for the stress σ_{rco} in the core, we will have:

$$\Delta n_{co} = -13.25 \cdot 10^{-6}\ \text{MPa}^{-1} \cdot \frac{\Delta T \cdot E_{co}}{2(1-\nu)} \left[\left(1 - \left(\frac{r_{co}}{r_{cl}} \right)^2 \right) \cdot (\alpha_{co} - \alpha_{cl}) \right] \tag{18}$$

In Eq. (18), we will replace the α_{co} with the mixed thermal expansion coefficient α_{mix} from Eq. (2) and the E_{co} with the mixed elastic modulus E_{mix} from Eq. (3). Then we will have the thermal stress-induced Δn-change in the core as a function of the material parameters, core radius, cladding radius and temperature change:

$$\Delta n_{co} = -13.25 \cdot 10^{-6} \cdot\ \text{MPa}^{-1} \cdot \frac{\Delta T \sum_i (x_i E_i)}{2(1-\nu)} \left[\left(1 - \left(\frac{r_{co}}{r_{cl}} \right)^2 \right) \cdot \left(\sum_i (c_i \cdot x_i \cdot \alpha_i) - \alpha_{SiO2} \right) \right] \tag{19}$$

where the parameters are defined similarly as in Eq. (6) and (9).

Equation (19) is our simplified model for the thermal stress-induced index change in a preform and in a fiber when we neglect the radial thermal distribution and cooling rate effects.

Next, we will add the draw induced mechanical stresses in the fiber model.

6. Stress-Induced Index Changes in Laser Fibers

Stresses in the optical fibers depend on dopant materials, fiber geometry, drawing tension, viscosities and temperature change ΔT. The modelled or the measured fiber stress values can be used as an input in the fiber refractive index change model. The measured stress values can be used for analysing index changes in existing fibers, and the modelled stress values are needed for predicting index changes in the new fiber designs.

The combined stress in a fiber consists of thermal stresses and mechanical stresses. The thermal stresses in the fibers are calculated in a similar way as in the preforms, Eq. (9), if we exclude the fiber cooling rate effects.

The drawing induced radial mechanical stress σ_{rm} in the fiber core depends on the fiber drawing tension σ_{zdr}, and on the core and cladding viscosities η_{co} and η_{cl} [21], [22], [26]. If the ratio of the viscosities $\eta_{co}/\eta_{cl} << 1$ and the elastic modulus values in the core and cladding are approximately equal ($E_{co} \approx E_{cl}$,) then the radial mechanical stress caused by different viscosities in the core and cladding can be approximated from the equations given in the ref. [21] by:

$$\sigma_{rm} = -1/2 \cdot \left(1 - \left(\frac{\eta_{co}}{\eta_{cl}} \right) \right) \cdot \sigma_{zdr} \tag{20}$$

The coefficient $-½$ (in the Eq. 20) comes from the Eq. (14). The η_{co} and η_{cl} are the viscosities of the core and cladding at the set point temperature of the undoped quartz. If the viscosity ratio η_{co}/η_{cl} is not $<<$ 1, then the complete equations in the ref. [21] need to be used. When the glass composition is known, the viscosities η_{co} and η_{cl} can be calculated with the viscosity models presented in the references [27], [28].

Combining the thermal stress σ_{rco} in Eq. (9) and the mechanical stress σ_{rm} in Eq. (20), the radial stress σ_{fr} in the fiber core is given by:

$$\sigma_{fr} = \frac{\Delta T \sum_i (x_i E_i)}{2(1-\nu)} \left[\left(1 - \left(\frac{r_{fco}}{r_{fcl}} \right)^2 \right) \cdot \left(\sum_i (c_i \cdot x_i \cdot \alpha_i) - \alpha_{SiO2} \right) \right] - 1/2 \cdot \left(1 - \left(\frac{\eta_{co}}{\eta_{cl}} \right) \right) \cdot \sigma_{zdr}, \tag{21}$$

where

σ_{fr} = residual axial stress in the fiber,
σ_{zdr} = drawing tension,

r_{fco} = radius of the fiber core,
r_{fcl} = radius of the fiber cladding.

When we know the combined radial stress in the fiber σ_{fr} in Eq. (21), we can calculate the stress-induced radial index change Δn_{fr} using Eq. (16). From Eq. (16) we have $\Delta n_{fr} = -13.25 \cdot 10^{-6} \times \text{MPa}^{-1} \cdot \sigma_{fr}$ and thus the stress-induced radial index change in the fiber core is:

$$\Delta n_{fr} = -13.25 \cdot 10^{-6} \cdot \text{MPa}^{-1} \cdot \left\{ \frac{\Delta T \cdot \sum_i (x_i \cdot E_i)}{2(1-\nu)} \left[\left(1 - \left(\frac{r_{fco}}{r_{fcl}} \right)^2 \right) \cdot \left(\sum_i (c_i \cdot x_i \cdot \alpha_i) - \alpha_{SiO2} \right) \right] - 1/2 \cdot \left(1 - \left(\frac{\eta_{co}}{\eta_{cl}} \right) \right) \cdot \sigma_{zdr} \right\} \quad (22)$$

7. Index Change Between a Preform and Fiber

Stress-induced radial index change Δn_{Sl} between a preform and fiber core is the difference of the stress-induced index change in the fiber core Δn_{fr} and in the preform core Δn_{pco}. The values are calculated using Eq. (22) and (19). The stress-induced index change between the two index profile measurements is then:

$$\Delta n_{Sl} = \Delta n_{fr} - \Delta n_{pco} \quad (23)$$

Combining Eq. (19) and (22) the index change Δn_{Sl} between the preform and fiber is:

$$n_{Sl} = -13.25 \cdot 10^{-6} \cdot \text{MPa}^{-1} \cdot \left\{ \frac{\Delta T \cdot \sum_i (x_i \cdot E_i)}{2(1-\nu)} \left[\left(\left(\frac{r_{pco}}{r_{pcl}} \right)^2 - \left(\frac{r_{fco}}{r_{fcl}} \right)^2 \right) \cdot \left(\sum_i (c_i \cdot x_i \cdot \alpha_i) - \alpha_{SiO2} \right) \right] - 1/2 \cdot \left(1 - \left(\frac{\eta_{co}}{\eta_{cl}} \right) \right) \cdot \sigma_{zdr} \right\}, \quad (24)$$

where

r_{pco} = radius of the preform core,
r_{pcl} = radius of the preform cladding.

If the core-cladding ratio is equal in the preform and fiber measurements, then only drawing induced stresses will change the Δn.

8. Results and Discussion

Figure 2 shows an example of a refractive index profile of a Yb-doped preform manufactured using DND technology, and a profile of a fiber drawn from the same preform. The preform index profile is measured using PK 2600 system and the fiber index profile using IFA-100 Fiber Refractive Index Profiler. Both index profiles are normalized in the radial direction.

The average index difference (Δn) values, first measured from the preforms and then measured from the fibers drawn from the same preforms, are compared in Fig. 3(a) and 3(b). Fig. 3(a) shows the original correlation between the index difference measurements of preforms and fibers. Fig. 3(b) shows the improved correlation when the modelled stress-induced index changes in the preforms and fibers are used to predict the change in the Δn values. When the modelled stress-induced index change values were combined with the measured preform index values, the correlation R^2 was improved from 82.7% (between the measured preform Δn_p and measured fiber Δn_f) to 97.5% (between the predicted fiber Δn_{fp} and measured fiber Δn_{fm}).

The preform index profiles were measured with PK 2600 preform index profiler. The drawn fibers were measured for their refractive index profiles using IFA-100 fiber refractive index profiler. According to the measurement instrument manufacturers, the repeatability of the (PK 2600) preform index profile value is $< 5 * 10^{-5}$, and refractive index accuracy of the (IFA-100) fiber index profiler is $\pm 1 * 10^{-4}$. The measured stress induced index changes are usually in the range of $(0 \ldots 5) *$

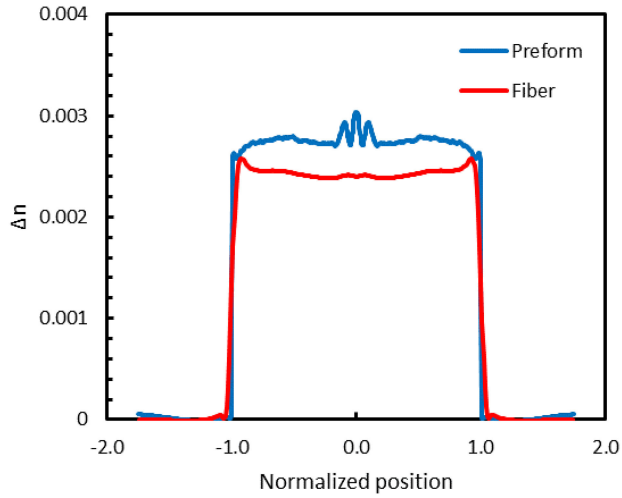

Fig. 2. Stress-induced refractive index change between a preform profile and the respective fiber profile.

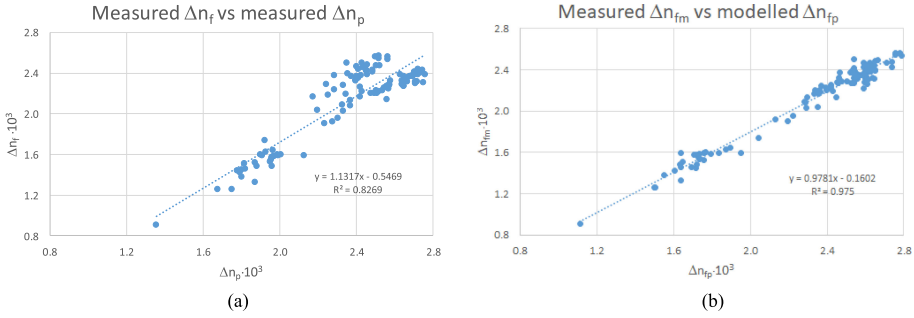

Fig. 3. (a) Correlation between the measured preform Δn_p and fiber Δn_f values. (b) Correlation between the modelled (predicted) Δn_{fp} and measured fiber Δn_{fm} values.

10^{-4}. The accuracy of the fiber index profiler is more limiting than the repeatability of the preform index profiler. Both systems are well calibrated, and they can detect the average index changes.

Instead of using full radial index profiles we compared radially and axially averaged refractive index difference values to make the analysis simpler. For the analysis we chose step-index type profiles; they are radially flat when manufactured with the DND-process.

9. Conclusions

Core Δn is one of the key factors determining a laser fiber performance (e.g., beam quality and mode field diameter). The smaller the standard deviation of the Δn distribution, the better the fibers can be matched and spliced with low losses.

In fiber manufacturing, the preform index profile is measured at the beginning, and the fiber index profile at the end of the production process. It is possible to predict the fiber Δn more accurately when we apply stress-induced index change model together with the measured preform Δn data. The improved fiber Δn estimates enable to fine-tune the preform and fiber manufacturing processes so that the Δn values of the drawn fibers will be close to the designed values.

A statistical model, presented in [5], can be applied reliably in the value space that was used to create the model, i.e., in a range where some measured data points exist. Stress-induced index change is based on a physical model that is not limited by existing measurement values [29]. The challenge of the stress-induced index change model is that the needed material parameter values

are functions of the temperature and in some cases depend nonlinearly on the concentrations. The published data of the material parameter values at high temperatures ($>$ 500C) is limited. Therefore, some estimations were needed in the high-temperature range. The improved correlations support the validity of the applied material parameter values and assumptions used in this model.

References

[1] G. W. Scherer, "Stress-induced index profile distortion in optical waveguides," *Appl. Opt.*, vol. 19, no. 12, pp. 2000–2006, 1980.

[2] H. Valkonen and P. Kiiveri, "Direct nanoparticle deposition technology for active fibres," *Int. Opt. Commun.*, 2002, pp. 2–3.

[3] S. Tammela *et al.*, "Direct nanoparticle deposition process for manufacturing very short high gain Er-doped silica glass fibers," in *Proc. 28th Eur. Conf. Opt. Commun.*, 2002, vol. 4, Paper 9.4.2.

[4] J. Koponen, L. Petit, T. Kokki, V. Aallos, H. Ihalainen, and J. Paul, "Progress in direct nanoparticle deposition for the development of the next generation fiber lasers," *Opt. Eng.*, vol. 50, no. 11, 2011, Art. no. 111605.

[5] P. Kiiveri *et al.*, "Predicting fiber refractive index from a measured preform index profile," *Proc. SPIE*, 10513, 2018, Art. no. 105131F.

[6] Y. Kikuchi, H. Sudo, and N. Kuzuu, "Thermal expansion of vitreous silica: Correspondence between dilatation curve and phase transitions in crystalline silica," *J. Appl. Phys.*, vol. 82, no. 8, pp. 4121–4123, 1997.

[7] *Thermal Properties of Fused Quartz*, Momentive Performance Materials, Inc., Waterford, NY, USA, 2016. [Online]. Available: https://www.momentive.com/en-US/categories/quartz/thermal-properties/. Accessed: Dec. 27, 2018.

[8] *NIST Property Data Summaries for Advanced Materials*, Nat. Inst. Standards Technol., Gaithersburg, MD, USA, 2002. [Online]. Available: https://srdata.nist.gov/CeramicDataPortal/Pds/Scdaos. Accessed: Jun. 15, 2018.

[9] S. Stecura and W. J. Campbell, "Thermal expansion and phase inversion of rare-earth oxides," U.S. Dept. Interior, Bureau of Mines, Washington, DC, USA, Rep. Investigations 5847, 1961.

[10] F. Just, H. Rainer-Müller, H. Bartelt, "Mechanical stresses in rare-earth doped fiber preforms," in *Proc. DGaO*, 2008. [Online]. Available: http://www.dgao-proceedings.de. Accessed: Dec. 20, 2018.

[11] J. F. Bacon, A. A. Hasapis, and J. W. Wholley Jr., "Viscosity and density of molten silica and high silica content glasses," *Phys. Chem. Glasses*, vol. 1, no. 3, pp. 90–98, 1960.

[12] J. L. Shackelford and W. Alexander, *CRC Materials Science and Engineering Handbook*, 3rd ed. Boca Raton, FL, USA: CRC Press, 2001, p. 1541.

[13] N. P. Bansal and R. H. Doremus, *Handbook of Glass Properties*. New York, NY, USA: Academic, 1986.

[14] M. Cavillon, P. D. Dragic, and J. Ballato, "Additivity of the coefficient of thermal expansion in silicate optical fibers," *Opt. Lett.*, vol. 42, no. 18, 3650–3653, 2017.

[15] F. Just, S. Unger, J. Kirchhof, V. Reichel, and H. Bartelt, "Thermal stress anomaly in rare-earth-doped fiber materials for high-power fiber lasers codoped with aluminum and phosphorus," *Proc. SPIE*, vol. 7721, 2010, Art. no. 772106.

[16] R. G. Munro, "Elastic moduli data for polycrystalline ceramics," Nat. Inst. Standards Technol., Gaithersburg, MD, USA, NISTIR Rep. 6853, 2002. [Online]. Available: https://srdata.nist.gov/CeramicDataPortal/scd. Accessed: Jun. 15, 2018.

[17] V. Rontu, A. Nolvi, A. Hokkanen, E. Haeggström, I. Kassamakov, and S. Franssila, "Elastic and fracture properties of free-standing amorphous ALD Al2O3 thin films measured with bulge test," *Mater. Res. Exp.*, vol. 5, no. 4, 2018, Art. no. 046411.

[18] P. D. Dragic, M. Cavillon, A. Ballato, and J. Ballato, "A unified materials approach to mitigating optical nonlinearities in optical fiber. II. B. The optical fiber, material additivity and the nonlinear coefficients," *Int. J. Appl. Glass Sci.*, vol. 9, pp. 307–318, 2018. https://doi.org/10.1111/ijag.12329.

[19] R. Le Parc, C. Levelut, J. Pelous, V. Martinez, and B. Champagnon, "Influence of fictive temperature and composition of silica glass on anomalous elastic behaviour," *J. Phys. Condens. Matter.*, vol. 18, no. 32, pp. 7507–7527, Aug. 2006.

[20] P. Kiiveri, A-M. Peder-Gothoni, and S. Tammela, Behaviour of fiber dopant materials in the MCVD-process, in *Proc. 12th Nordic Semicond. Meet.*, 1986, pp. 335–338.

[21] P. K. Bachmann, W. Hermann, H. Wehr, and D. U. Wiechert, "*Stress in optical waveguides. 2. Fibers*," *Appl. Opt.*, vol. 26, pp. 1175–1182, 1987.

[22] P. K. Bachmann, W. Hermann, H. Wehr, and D. U. Wiechert, "Stress in optical waveguides. 1. Preforms," *Appl. Opt.*, vol. 25, pp. 1093–1098, 1986.

[23] L. Pagnotta and A. Poggialini, "Measurement of residual internal stresses in optical fiber preforms," *Exp. Mechanics*, vol. 43, no. 1, pp. 69–76, 2003.

[24] A. D. Yablon, "Optical and mechanical effect of frozen-in stresses and strains in optical fibers," *IEEE J. Sel. Top. Quantum Electron.*, vol. 10, no. 2, pp. 300–311, Mar./Apr. 2004.

[25] W. Hermann, M. Hutjens, and D. U. Wiechert, "Stress in optical waveguides 3: Stress induced index change," *Appl. Opt.*, vol. 28, no. 11, pp. 1980–1983, 1989.

[26] F. Just, R. Spittel, J. Bierlich, S. Grimm, M. Jäger, and H. Bartelt, "The influence of the fiber drawing process on intrinsic stress and the resulting birefringence optimization of PM fibers," *Opt. Mater.*, vol. 42, pp. 345–350, 2015.

[27] M. I. Ojovan, "Viscosity and glass transition in amorphous oxides," *Adv. Condens. Matter. Phys.*, vol. 2008, 2008, Art. no. 817829.

[28] Y. Bottinga, P. Richet, and A. Sipp, "Viscosity regimes of homogenous silicate melts," *Amer. Mineralogist*, vol 80, pp. 305–318, 1995.

[29] P. Kiiveri *et al.*, "Stress induced refractive index changes in preforms and laser fibers," *Proc. SPIE*, vol. 10897, 2019, Art. no. 1089727.